The influence of the structure (surface roughness, pore size, and porosity) of 3D printed silk-fibroin-based scaffolds on the growth of the bronchial epithelial cells *in vitro*

Nongping Zhong
The First Affiliated Hospital of Nanchang University
Zhongchun Chen
Huashan Hospital of Fudan University
Tao Dong
Fudan University
Zhengzhong Shao
Fudan University
Xia Zhao (zhaoxiaabc@126.com)
Huashan Hospital of Fudan University

Research Article

Keywords: Silk fibroin, 3D printing, airway epithelial cell, surface morphology, porosity

Posted Date: April 13th, 2022

DOI: https://doi.org/10.21203/rs.3.rs-1529862/v1

Abstract

The structure (surface topography, pore size, and porosity) of 3D scaffolds plays an important role in tissue regeneration. Although surface topography, the porosity and pore size of 3D porous scaffolds have been frequently studied, these parameters of 3D printed SF-based scaffolds for tracheal epithelium growth have not been investigated. In this study, we investigated the effects of the structure properties of 3D printed silk fibroin/Hydroxypropyl methyl cellulose(SF/HPMC) scaffolds on the adhesive and proliferative behaviors of tracheal epithelium in vitro. This work fabricated six types of 3D printed SF/HPMC scaffolds with different surface properties, pore size and porosity. The surface topography, pore size, and porosity of the different scaffolds were examined. Normal human bronchial epithelial cell lines (BEAS-2B cells) were cultured on the different scaffolds for 7 days. The proliferation of cells on the different scaffolds was tested by CCK-8 assay. The morphology of BEAS-2B cells on different scaffolds was observed by scanning electron microscopy(SEM). The porosity of 20 wt% SF/HPMC scaffolds with rough surface and smooth surface, and 30 wt% SF/HPMC scaffolds with rough surface and smooth surface were 70.5 ±2.0% 65.5 ±6.1% 63.9 ±2.1% 59.6 ±2.1%, respectively; The pore size of 20 wt% SF/HPMC scaffolds was 443.9±104.1μm and 681.1±115.1μm, respectively. Results showed that BEAS-2B cells proliferated better on the rough surface than that on the smooth surface; BEAS-2B cells proliferated better on the scaffold with higher porosity (65.5 ±6.1%) than that with lower porosity (59.6 ±2.1%); In addition, the cells proliferated well on the SF/HPMC scaffold with small pore size (443.9±104.1μm). SEM showed that cells grew in a sheet on the rough surface and tended to grow in clusters on the smooth surface; BEAS-2B cells tended to grow in clusters on the scaffold with large pore size, while cells could spread into a sheet and form connections between pores on the scaffold with small pore size. In summary, SF/HPMC scaffolds with rough surface, high porosity, and small pore size facilitated cell growth. This provides a preliminary experimental basis for selecting the suitable structure of 3D printed SF/HPMC scaffolds for repairing tracheal defects.

Background

Tissue engineering, a multidisciplinary field, has the potential to restore, maintain, and enhance tissue and organ functions [1]. The scaffolds are essential in tissue engineering as they can provide an environment for supporting cell adhesion, proliferation and differentiation to form the new tissues and organs[2]. In addition, the scaffold should facilitate the nutrient diffusion, removal and exchange of metabolic substances during cell culture [3,4]. Thus, a proper scaffold is critical in tissue engineering. An ideal tissue engineered scaffold should have the following demands: biocompatibility, biodegradability with a controllable degradation rate, three dimensional (3D) and porous structure to promote cell migration and transportation of nutrients, oxygen, and waste products, a suitable surface for cell attachment and proliferation, and good mechanical properties [5].

Natural polymers (collagen, gelatin, chitosan, etc.) have been widely used for tissue engineering due to their good biocompatibility [6–8]. However, these polymers have certain limitations such as poor

mechanical strength, rapid degradation, etc. [9]. Silk fibroin (SF), one of natural macromolecular protein polymer, has been used in various biotechnological and biomedical applications because of its good biocompatibility, outstanding mechanical properties and controllable degradation rates [10–11]. Through different treatment, SF can be formed the diverse structure such as fiber, film, and three dimensional porous structures which could promote the growth of fibroblasts, cartilage, mesenchymal stem cells, epithelial cells, etc. [3,12]. In general, 3D porous scaffolds could mimic in vivo microenvironments and facilitate the nutrients transport, which can support cell adhesion and proliferation [5]. SF could form the 3D porous structures by traditional methods. However, traditional methods of fabricating 3D porous scaffolds are difficult to exactly control their structure and internal geometry [13]. Recently, we could fabricate the 3D porous scaffolds layer by layer with computer-controlled repetition of desired structures by using 3D printing [14,15].

Clinically, the repair of trachea was difficult as it is exposed to the outside environment, which make it difficult for epithelial regeneration. Thus, the scaffold used for repairing the trachea defect should facilitate the growth of tracheal epithelium [16]. Previously, our group made the 3D porous SF scaffold by a traditional method of freezing-defrosting process for repairing tracheal defect and results showed that the 3D porous SF scaffold could promote the proliferation of tracheal epithelial cells. Furthermore, to precisely control the structure of the scaffold, we used SF and hydroxypropyl methylcellulose (HPMC) which is a kind of cellulose ether derivatives to fabricate the 3D SF/HPMC scaffold by 3D printing. In vitro experiments showed that the BEAS-2B cells could proliferate on the 3D printed SF/HPMC scaffold[17]. However, the effect of the properties (such as surface roughness, pore size, and porosity) of 3D printed SF/HPMC scaffolds on tracheal epithelial cells was unknown. And to our knowledge, there is no report about the influence of 3D printed scaffold properties on tracheal epithelial cells. These parameters of scaffold can affect cell adhesion, migration and proliferation [3,18,19].

In this study, we investigated the appropriate parameters (surface roughness, pore size, and porosity) of 3D printed SF/HPMC scaffold for the growth of tracheal epithelial cells. We fabricated the different porosity of 3D printed SF/HPMC scaffolds by using the different concentration of SF/HPMC solution and the surface roughness was made by freezing process [20]. SF/HPMC scaffolds with various pore sizes were fabricated by adjusting the printing parameters. Then the attachment and proliferation of tracheal epithelial cells on different parameters of 3D printed SF/HPMC scaffolds were assessed. It is hoped that this study could provide reference data for the development of artificial tracheal grafts.

Results And Discussion

Scaffold fabrication

It is well known that the 3D porous scaffolds parameters such as surface topography, pore size, and porosity could influence the cell survival and proliferation. Over the years, many methods have been devised and investigated to promote cell attachment and subsequent cell proliferation on scaffolds by

changing the surface topography, pore size, and porosity [3, 19, 21]. Besides, with the development of 3D printing, we could fabricate the 3D porous scaffolds with better controlled structure. In the process of 3D printing SF/HPMC scaffolds, we combined the age-old technique of freeze-drying method[22] to make the scaffolds having micro-pores in the printed single filament. However, we observed that the surface of the 3D printed SF/HPMC scaffolds was smooth after freeze-drying. As the cell adhesion and proliferation can be influenced by subtle changes in microtopography, and different cell types have been shown a preference for either a smooth or a rough topography[23]. Changing surface microtopography can influence cellular responses in vitro and if they are negatively affected, it could not be suitable for implantation [24]. Therefore, we tried to fabricate the 3D printed SF/HPMC scaffolds with different surface topography. As the mixture of SF and HPMC could develop a hydrogel with the formation of small and uniform β-sheet structure after heating at 70℃ for 1h [25], which would not dissolve in water, we assumed that if the 3D printed SF/HPMC hydrogel was sprayed water after the 3D printing and then frozen at -20℃ for 24h before freeze-drying, the ice crystals formed on the surface of the scaffold could make the surface rough. Results showed that 3D printed SF/HPMC scaffolds with spraying water had the rougher surface than that of scaffolds without spraying water. The choice of freeze-drying as a surface modifying method described herein had several advantages. This method is simple and do not require some chemicals as the ice crystals formed during freezing can be removed simply by sublimation.

SF/HPMC scaffold characterization

Scanning electron microscopy (SEM)

SEM was used to observe the morphology and pore size of the scaffold. The 20% SF/HPMC scaffold with spraying water had a rougher surface than that of 20% SF/HPMC scaffold without spraying water. There were some cracks on the surface of 20% SF/HPMC scaffold with spraying water. The surface of the 30% SF/HPMC scaffold with spraying water was rough and formed the shape of the grid. Its surface was rougher than other three groups. The surface of the 30% SF/HPMC scaffold without spraying water was the smoothest among the four groups. Images showed that there was similar surface topography between 20% SF/HPMC scaffold without spraying water and 30% SF/HPMC scaffold without spraying water (Fig. 1A-H). The cross- section images showed that four types of scaffolds had micro-scale pores in the cross section. The 20% SF/HPMC scaffold with spraying water had a similar pore structure to the 30% SF/HPMC scaffold with spraying water, which there were tiered holes in the section. Moreover, the 20 wt% SF/HPMC scaffold with spraying water has a thinner hole wall structure than the 30 wt% SF/HPMC scaffold without spraying water, and the connectivity of the holes was higher than that of the 30 wt% SF/HPMC scaffold (Fig. 1H, J). The cross-sectional pore size of the 20 wt% SF/HPMC scaffold without water spraying was larger than that of the 30 wt% SF/HPMC scaffold without water spraying, and the hole wall is thinner than the 30 wt% SF/HPMC scaffold without water spraying (Fig. 1I, K).

To investigate the influence of pore size on cell proliferation, the 3D printed 20% SF/HPMC scaffold with spraying water was used. The morphology of 3D printed SF/HPMC scaffolds with two different pore

sizes was shown in Fig. 1L, M. The diameter of macro-pores of two scaffolds, which were the distance between the single printed filament, were 681.1$\pm$115.1μm and 443.9$\pm$104.1um, respectively.

Porosity and water content of SF/HPMC scaffolds

The porosity of 20 wt% SF/HPMC scaffold with spraying water, 20 wt% SF/HPMC scaffold without spraying water, 30 wt% SF/HPMC scaffold with spraying water, and 30 wt% SF/HPMC scaffold without spraying water was 70.5 ± 2.0%, 65.5 ± 6.1%, 63.9 ± 2.1% and 59.6 ± 2.1%, respectively. There were significant differences between 20% SF/HPMC scaffold and 30% SF/HPMC scaffold. In the same concentration of SF/HPMC scaffolds, the porosity of spraying water was higher than that of without spraying water, but no significant difference was found. And the water content of 20 wt% SF/HPMC scaffold with spraying water, 20 wt% SF/HPMC scaffold without spraying water, 30 wt% SF/HPMC scaffold with spraying water, and 30 wt% SF/HPMC scaffold without spraying water was 80.5±±0.8%, 79.9±0.53%, 77.1±0.7% and 68.8±2.3%, respectively. There were significant differences between 20% SF/HPMC scaffold and 30% SF/HPMC scaffold of water content. In the same concentration of SF/HPMC scaffolds, water content of spraying water was high than that of without spraying water (Fig. 2A, B).

The porosity of 20% SF/HPMC scaffolds with large pore was higher than that of small pore. The water uptake of 20% SF/HPMC scaffolds with large pore was lower than that of small pore. There were no significant differences between two groups of porosity and water content (Fig. 2C, D).

In vitro evaluation

BEAS-2B cells proliferation and viability on different scaffolds

Cell proliferation and viability on different kinds of SF/HPMC scaffolds were invested by CCK-8 assay. Cell proliferation results showed that BEAS-2B cells on 3D printed porous scaffolds with rough surface proliferated well than those on scaffolds with smooth surface, indicating that the scaffolds with rough surface could offer a favorable environment for BEAS-2B cells adhesion, proliferation, and migration (Fig. 3A). Furthermore, the behavior of cells may also be influenced by different topographic sizes, ranging from macroscale to microscale and nanoscale features[26]. The prepared 30% SF/HPMC scaffold with spraying water had the morphology of microscale grid on the surface and this structure facilitated the BEAS-2B cells attachment compared with those grown on the smooth surfaces, which was similar with the osteoblast [27].

In addition, the porosity and pore size of the scaffolds play a crucial role in cell growth and tissue formation. Porosity and interconnection within the scaffolds are necessary to distribute oxygen as well as nutrients [28]. Combined with freeze-drying method, we obtained the 3D printed SF/HPMC scaffolds having multi-level pores including macro-pores and micro-pores. The diameter of macro-pores could be controlled by changing the distance between printed filaments through computer. Besides, previous study showed that the concentration of SF solution had a crucial influence on the pore size and porosity of the

SF scaffolds [20]. Therefore, Micro-pores in the printed single filament of SF/HPMC scaffolds could be altered by changing the concentration of SF. Results showed that the porosity of prepared 20% SF/HPMC scaffolds was higher than that of 30% SF/HPMC scaffolds. Cell proliferation on four types of 3D printed SF/HPMC scaffolds showed some very interesting results. It was observed that cell proliferation on 20% SF/HPMC scaffolds with high porosity was good than that of 30% SF/HPMC scaffolds with smooth surface. However, compared with 20% SF/HPMC scaffolds, the 30% SF/HPMC scaffold with rough had a lower porosity, but with the best cell proliferation, suggesting that the rough surface of scaffolds might be more important for BEAS-2B cells attachment and proliferation than porosity.

The 3D printed SF/HPMC scaffolds with the different pore size were fabricated by adjusting the distance between the filaments during the printing process. From the above findings, we found that the 20% SF/HPMC scaffold with rough surface facilitated the cell attachment and growth. Thus, 20% SF/HPMC solution was chosen to fabricate the scaffolds with the different pore size. It was observed that cell on the scaffold with small pore size proliferated better than that on scaffolds with large pore size (Fig. 3B). This may be due to more liquid could pass through and leave the scaffold with high pore size. This result was in agreement with the previous studies with 3D printed scaffold [27]. In generally, too small pore sizes could limit the transport of nutrients and cell proliferation and pore sizes above 300um could facilitate the vascularized tissue formation [29]. However, if the pores are too large, the decrease in surface area limits cell adhesion. Therefore, pore size should be within a proper range to maintain the balance between the optimal pore size for cell proliferation, nutrients transportation, vascularization and specific surface area for cell attachment as well as mechanical stability [5].

The BEAS-2B cells viability on different kinds of SF/HMPC scaffolds was further analyzed by live/dead staining. The images showed that BEAS-2B cells on four types of SF/HPMC scaffolds keep live at 1, 3, and 7 days (staining green) (Fig. 3C). No dead cells were found during the culturing period (staining red). The cells proliferate along the single printed filament. In addition, BEAS-2B cells on different pore size of SF/HPMC scaffolds showed good viability at 1, 3 and 7 days. Most of cells were live and stained by calcein-AM.

Cell attachment and morphology

Cell morphology on different scaffolds were studied by SEM. Images showed that cells could attached on the four types of SF/HPMC scaffolds, however, lots of cells attached on the scaffold with rough surface (20% and 30% SF/HPMC scaffold with spraying water) at day 1. And cells on the four types of scaffolds were scattered and isolated. They did not stretch their microfilaments and cytoskeleton completely. At day 3 and 7, SEM showed that cells grew in a sheet on the rough surface and tended to grow in clusters on the smooth surface (Fig. 4A-L); At day 7, cells on scaffolds with small pore size proliferated along the surface of scaffolds and formed cell bridging between the printed filaments (Fig. 4N, P). In addition, cells on the 3D printed SF/HPMC scaffolds with large pores liked to aggregate on the side wall of large pores (Fig. 4M, O), and were difficult to form a bridge between the filaments, which was inappropriate for 2D tissues such as epithelium [29].

Conclusions

In this study, we fabricated the 3D porous SF/HPMC scaffolds by 3D printing and investigated the suitable scaffolds parameters (surface roughness, porosity, and pore size) for tracheal epithelium growth. The 3D-printed porous SF/HPMC scaffold combined with vacuum freeze-drying technology formed a structure with rough surface, small pore size, and suitable porosity, which was beneficial to the exchange of nutrients and metabolites and is conducive to the attachment and proliferation of BEAS-2B cells. These indicate that the 3D printed SF/HPMC scaffold with these properties showed its potential as a suitable scaffold for tracheal epithelium regeneration.

Materials And Methods

Preparation of SF and HPMC aqueous solution

The aqueous SF solution was prepared as described previously [20]. Briefly, sericin in cocoon of *B. mori* silkworm was removed by boiling in Na_2CO_3(0.5 wt%) aqueous solution for 45 min. Then the SF was washed with distilled water and dried at 37℃. Dried silk fibroin was dissolved in 9.3 mol/L LiBr solution at 60℃ for 1h. After been dialyzed for three days, the SF solution was dialyzed against polyethyleneglycol (PEG) (PEG20000, Ourchem, China) solution and the concentration of 30–32 wt% SF solution was obtained. Then the concentrated solution was diluted to 20 wt% and 30 wt% with deionized water respectively. HPMC powders (Aladdin, China) were dissolved in deionized water to form a 10 wt% solution.

Scaffold fabricating

To obtain the different porosity of 3D printed SF/HPMC scaffolds, the different concentration of SF solution (20 wt% and 30 wt%) was used. Scaffolds with different degrees of roughness were prepared by spraying water on the surface of the scaffold during the printing process and combining the freezing process; 20 wt% SF/HPMC scaffolds of two different pore sizes were prepared by adjusting the printing parameters.The 10 wt% HPMC solution was added to 20 wt% and 30 wt% SF solutions, respectively. The volume ration of SF to HPMC was 9:1. Two mixture (20% SF/HPMC and 30% SF/HPMC) were poured into nozzles of the 3D printer and then transferred to a gel state at 70℃ for 1 h. 3D SF/HPMC scaffolds with pre-determined shape and dimension were fabricated by using a 3D bioprinting machine (Regenovo 3D Bio-printer, China). The 20% SF/HPMC and 30% SF/HPMC scaffolds were printed into a square shape. Six kinds of 3D printed SF/HPMC scaffolds were fabricated (20% SF/HPMC with smooth surface, 20% SF/HPMC with rough surface, 30% SF/HPMC with smooth surface, 30% SF/HPMC with rough surface, 20% SF/HPMC with small pore size and 20% SF/HPMC with large pore size). To obtain the rough surface of scaffolds, the scaffolds were sprayed water by using sprinkling can after the fabrication process. Then all scaffolds were frozen at -20℃ for 24h and freeze-dried for 2 days. At last, freeze-dried 3D printed scaffolds were immersed in 75% ethanol for 1 hour at room temperature for further formation of stable β-sheet structure. The pore size of 3D printed SF/HPMC scaffolds was determined by the spacing between

the filaments extruded from the nozzle. To fabricate the different pore size of 3D printed SF/HPMC scaffolds, 20% SF/HPMC mixture was used and the scaffolds were sprayed water after the completion of printing. According to adjusting the spacing of printing by software, scaffolds with two different pore sizes were constructed.

Scaffold characterization

Morphology of the 3D printed SF/HPMC scaffolds

The surface morphology and pore size of 3D printed SF/HPMC scaffolds were investigated using a scanning electron microscopy (SEM) (Hitachi S4800 microscope, Japan). The surface and cross sections of SF/HPMC scaffolds were coated with Au and then observed by SEM (n = 3 per group). Image J software was used to measure the diameter of the pore size of 3D printed scaffolds.

Porosity measurement

The porosity of 3D printed SF/HPMC scaffolds were measured according to liquid displacement method using hexane which is a non-solvent of SF [30]. The porosity was calculated according to the following formula: Porosity = $[(V_1-V_3)/(V_2-V_3)] \times 100\%$ (n = 5 per group), where V_1 is the volume of hexane, V_2 is the total volume of the hexane and 3D printed SF/HPMC scaffolds impregnated with the hexane, and V_3 is the volume of the remained hexane which the hexane impregnated SF/HPMC scaffolds were removed.

Water uptake

The water uptake and the water content of the 3D printed SF/HPMC scaffolds were calculated as follows (n = 5 per group):

Water uptake= (W1-W2) / W2

Water content (%) = [(W1-W2)/ W1] ×100%

The 3D printed SF/HPMC scaffolds were immersed in distilled water for 24h. W1 represents the wet weight of the scaffold. W2 represents the dry weight of the scaffold.

The results were presented with the average of five scaffolds.

In vitro evaluation

Cell proliferation on 3D printed SF/HPMC scaffolds

BEAS-2B cells (ATCC, USA) proliferation on 3D printed SF/HPMC scaffolds were assessed by CCK-8 assay analysis. The six types (20% SF/HPMC with smooth surface, 20% SF/HPMC with rough surface, 30% SF/HPMC with smooth surface, 30% SF/HPMC with rough surface, 20% SF/HPMC with small pore size and 20% SF/HPMC with large pore size) of printed SF/HPMC scaffolds were used. The printed SF/HPMC scaffolds with the size of 5mm length ×5 mm width × 2mm height were put in 48-well plates.

The 20 ul of BEAS-2B cells suspension containing about 4.5×10^4 cells were seeded on the scaffolds. After half an hour, the fresh Dulbecco's Modified Eagle Medium (DMEM) (Hyclone, USA) medium containing 10% fetal bovine serum (10% FBS) and 1% penicillin and streptomycin (Hyclone, USA) was added into each well. After 1, 3, 5 and 7 days, scaffolds were transferred to a new 48-well plate. And then 200 ul of medium containing 50 ul CCK-8 solution was added and incubated for 3 h at 37 ℃ with 5% of CO2. Then, the solution (100 μL) was pipetted into a 96-well plate, and the absorbance at 450 nm was measured using a microplate reader (Bio-Tek Instruments, USA). Six scaffolds of each group were used for each culture period.

Cell morphology on 3D printed SF/HPMC scaffolds

The morphology and proliferation of BEAS-2B cells on four types and three different pore sizes of printed SF/HPMC scaffolds were observed by SEM (Hitachi SU8000 microscope, Japan). The BEAS-2B cells were seeded and cultured for 7 days. After cultured for 1, 3, and 7 days, the cell-scaffold constructs of each group were washed with phosphate-buffered saline (PBS) and were fixed in 2.5% glutaraldehyde for at least 24 hours at 4°C. Then the scaffolds were dehydrated using a graded series of ethanol. After being critical-point dried in carbon dioxide and coated with gold platinum, the cell-scaffold constructs were observed with SEM at an accelerating voltage of 10 kV.

Cell viability on 3D printed SF/HPMC scaffolds

The viability of BEAS-2B cells on six types of printed SF/HPMC scaffolds was further investigated by live/dead assay (Sigma, USA). The prepared SF/HPMC scaffolds with the same size of the above were put in 48-well plates. The BEAS-2B cells were suspended in the culture medium and 20 ul cell suspension containing 10×10^4 cells were seeded into scaffolds. The cell-scaffold constructs were added with 200 ul medium after being incubated for half an hour to allow cell to adhere. After 1, 3, 7 days, 20 uM calcein-AM (staining live cells) and 1ug/ml propidium iodide (PI, staining dead cells) in PBS were added and incubated for 20 min at 37°C. The cell-scaffold constructs of each group were imaged by confocal laser scanning microscopy (CLSM) (Leica, Germany) at certain wavelengths of 488 nm (Calcein-AM) and for 535 nm (PI).

Declarations

Authors Contributions

NZ and ZC performed the experiments and wrote the manuscript. NZ and ZC contributed equally to this manuscript. XZ and ZS supervised the work. TD participated in scaffold preparation and analyses. All authors contributed to the article and approved the submitted version.

Funding

The author(s) disclosed receipt of the following financial sup- port for the research, authorship, and/or publication of this article: This work was financially supported by Shanghai Science and Technology

Committee (Grant Number 17441901600), Shanghai Natural Science Foundation (Grant Number 19ZR1407700) and Application cultivation plan of Jiangxi Provincial department of science and technology (Grant Number 20212BAG70013).

Availability of data and materials

The datasets used and/or analysed during the current study available from the corresponding author on reasonable request.

Ethics approval and consent to participate

This study was approved by Ethical Board of Huashan Hospital, Fudan University.

Conflicting Interests

The author(s) declared no potential conflicts of interest with respect to the research, authorship, and/or publication of this article.

References

1. Vacanti JP, Langer R. Tissue engineering: the design and fabrication of living replacement devices for surgical reconstruction and transplantation. *Lancet* 1999;354 Suppl 1:S32-S34.
2. Lu H, Kawazoe N, Kitajima T, et al. Spatial immobilization of bone morphogenetic protein-4 in a collagen-PLGA hybrid scaffold for enhanced osteoinductivity. *Biomaterials* 2012;33:6140-6.
3. Han KS, Song JE, Tripathy N, et al.Effect of Pore Sizes of Silk Scaffolds for Cartilage Tissue Engineering. *Macromolecular Research* 2015;23:1091-1097.
4. Silva MM, Cyster LA, Barry JJ, et al. The effect of anisotropic architecture on cell and tissue infiltration into tissue engineering scaffolds. *Biomaterials* 2006;27:5909-5917.
5. Kress S, Neumann A, Weyand B, et al. Stem Cell Differentiation Depending on Different Surfaces.*Adv Biochem Eng Biotechnol* 2012;126:263-83.
6. Nelda Vázquez-Portalatı N, Kilmer CE, Panitch A, et al. Characterization of Collagen Type I and II Blended Hydrogels for Articular Cartilage Tissue Engineering.*Biomacromolecules* 2016;17:3145-3152.
7. Rodríguez-Vázquez M, Vega-RuizB, Ramos-Zúñiga Chitosan and Its Potential Use as a Scaffold for Tissue Engineering in Regenerative Medicine.*Biomed Res Int* 2015;821279.
8. Baiguera S, Gaudio CD, Lucatelli E, et al.Electrospun gelatin scaffolds incorporating rat decellularized brain extracellular matrix for neural tissue engineering.*Biomaterials* 2014;35:1205-1214.
9. Kasoju N, Bora U.Silk Fibroin in Tissue Engineering. *Advanced healthcare materials* 2012;1:393-412.
10. Melke J, Midha S, Ghosh S, et al. Silk fibroin as biomaterial for bone tissue engineering. *Acta Biomater* 2016;31:1-16.

11. Kapoor S, Kundu SC. Silkprotein-based hydrogels: Promising advanced materials for biomedical applications.*Acta Biomater* 2016;31:17-32.
12. Lin S, Lu G, Liu S, et al. Nanoscale control of silks for nanofibrous scaffold formation with an improved porous structure. *J Mater Chem B* 2014; 2(17):2622-2633.
13. Qi Y, Wang H, Wei k, et al. A Review of Structure Construction of Silk Fibroin Biomaterials from Single Structures to Multi-Level Structures. *Int J Mol Sci* 2017;18:237.
14. Sun L, Parker ST, Syoji D, et al. Direct-Write Assembly of 3DSilk/Hydroxyapatite Scaffolds for Bone Co-Cultures. *AdvHealthc Mater* 2012;1: 729-735.
15. Lee H, Yang GH, Kim M, et al. Fabrication of micro/nanoporouscollagen/dECM/silk-fibroin biocomposite scaffolds using a low temperature 3D printing process for bone tissue regeneration. *Mater SciEng C Mater BiolAppl* 2018;84:140-147.
16. Park JH, Park JY, Nam IC, et al. Human turbinate mesenchymal stromal cell sheets with bellows graft for rapid tracheal epithelial regeneration.*Acta Biomater* 2015;25:56-64.
17. Zhong NP, Dong T, Chen ZC, et al. A novel-3D-printed silk fibroin-based scaffold facilitates tracheal epithelium proliferation in vitro. Journal of biomaterials applications 2019;34:3-11.
18. Yang G, Lee H, Kim G. Preparation and characterization of spiral-like micro-struts with nano-roughened surface for enhancing the proliferation and differentiation of preosteoblasts. *Journal of industrial and engineering chemistry* 2018;61:244-254.
19. He FL, Li DW, He J, et al. A novel layer-structured scaffold with large pore sizes suitable for 3D cell culture prepared by near-field electrospinning. *Mater Sci Eng C Mater Biol Appl* 2018;86:18-27.
20. Cao Z, W J, Yao J, et al. Facile fabrication of the porous three-dimensional regenerated silk fibroin scaffolds. *Mater Sci Eng C Mater Biol Appl* 2013;33:3522-3529.
21. Crowley C, Klanrit P, Butler C, et al.Surface modification of a POSS-nanocomposite material to enhance cellular integration of a synthetic bioscaffold.*Biomaterials* 2016;83:283-293.
22. Deville S, Saiz E, Nalla RK, et al. Freezing as a path to build complex composites. *Science* 2006;311:515–518.
23. Tengvall P, Brunette DM, Textor M, et al. Principles of cell behavior on titanium surfaces and their application to implanted devices. *Springer* 2001; 485-512.
24. Hayes JS, Czekanska EM, Richards RG. The Cell–Surface Interaction. *Tissue Engineering III: Cell-Surface Interactions for Tissue Culture* 2011;126:1-31.
25. Luo K, Yang Y, Shao Z. Physically Crosslinked Biocompatible Silk-Fibroin-Based Hydrogels with High Mechanical Performance. *Adv Func Mater* 2016;26:872-880.
26. Lincks J, Boyan BD, Blanchard CR, et al.Response of MG63 osteoblast-like cells to titanium and titanium alloy is dependent on surface roughness and composition. *Biomaterials* 1998;19:2219-2232.
27. Roosa SMM, Kemppainen JM, Moffitt EN, et al.The pore size of polycaprolactone scaffolds has limited influence on bone regeneration in an in vivo model. *J Biomed Mater Res Part A* 2010;92A:359-

368.

28. Ruiz-Cantu L, Gleadall A, Faris C, et al. Characterisation of the surface structure of 3D printed scaffolds for cell infiltration and surgical suturing. *Biofabrication* 2016;8:015016.
29. McHugh KJ, Tao SL, Saint-Geniez M. A Novel Porous Scaffold Fabrication Technique for Epithelial and Endothelial Tissue Engineering. *J Mater Sci Mater Med* 2013; 24:1659-1670.
30. Kim UJ, Park J, Kim HJ, et al. Three-dimensional aqueous-derived biomaterial scaffolds from silk fibroin. *Biomaterials* 2005;26:2775-2785.

Figures

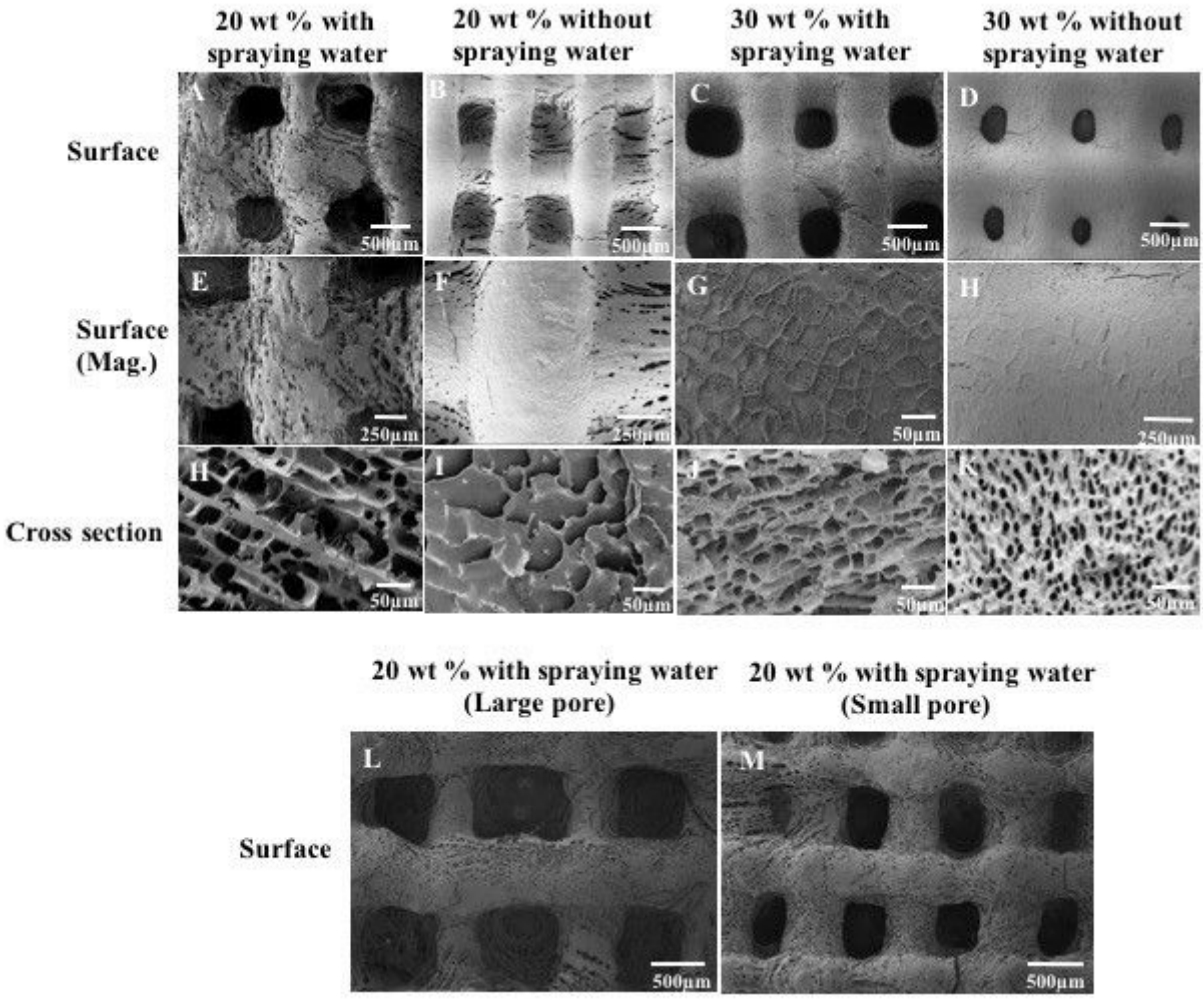

Figure 1

SEM images of six types of SF/HPMC scaffolds. **(A-D)** The surface morphology of scaffolds. **(E-H)** Magnified image of the 3D printed SF/HPMC bar. **(H-K)** Cross-sectional morphology of scaffolds. **(L-M)** The surface morphology of scaffolds with different pore sizes.

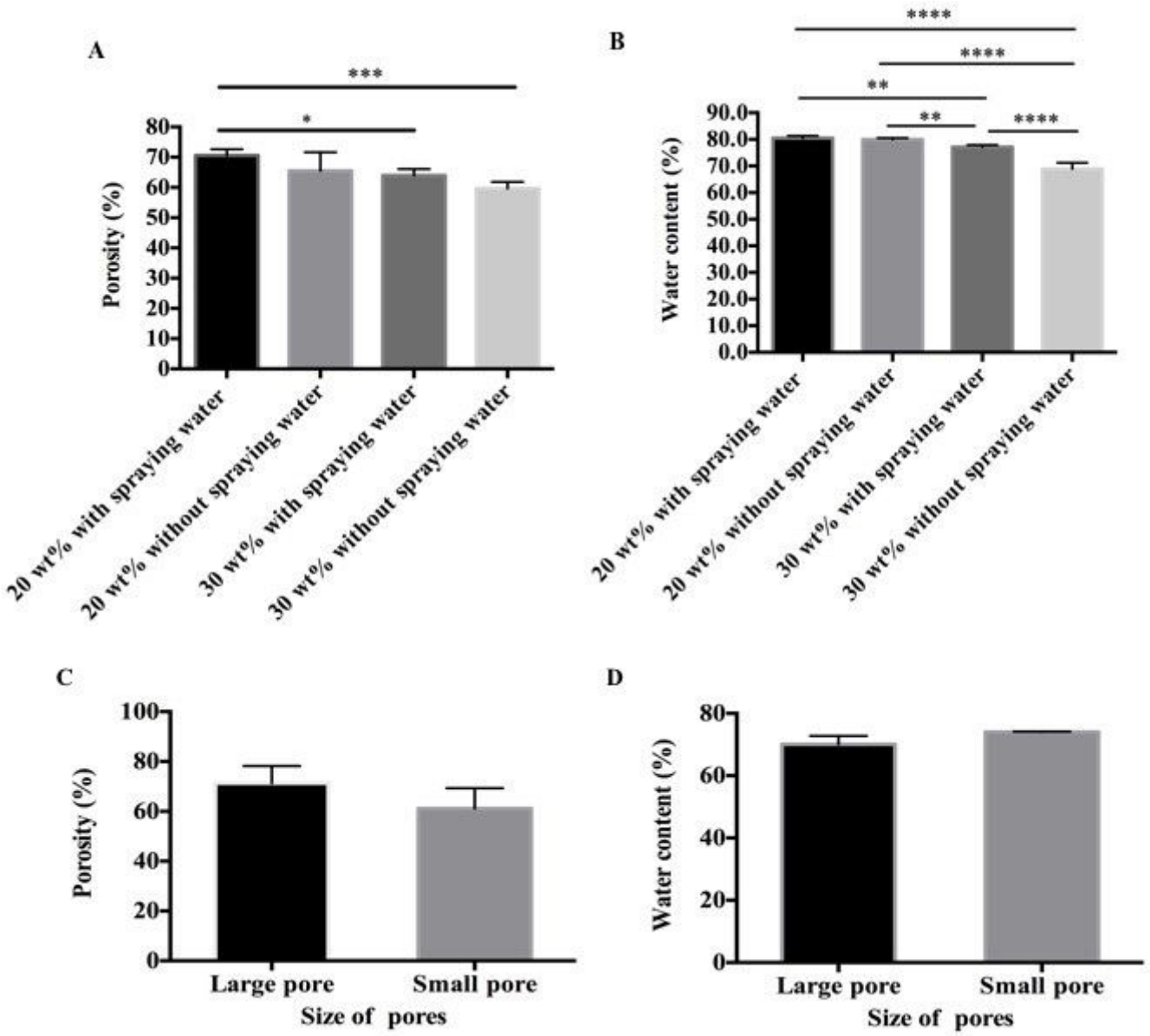

Figure 2

The porosity and water content of six types of scaffolds. **A** The porosity of four types of scaffolds. **B** The water content of four types of scaffolds. * denotes P < 0.05, ** denotes P < 0.01, *** denotes P < 0.001, **** denotes P < 0.0001. **C** The porosity of 20% SF/HPMC scaffolds with large pore and small pore. **D** The water content of 20% SF/HPMC scaffolds with large pore and small pore.

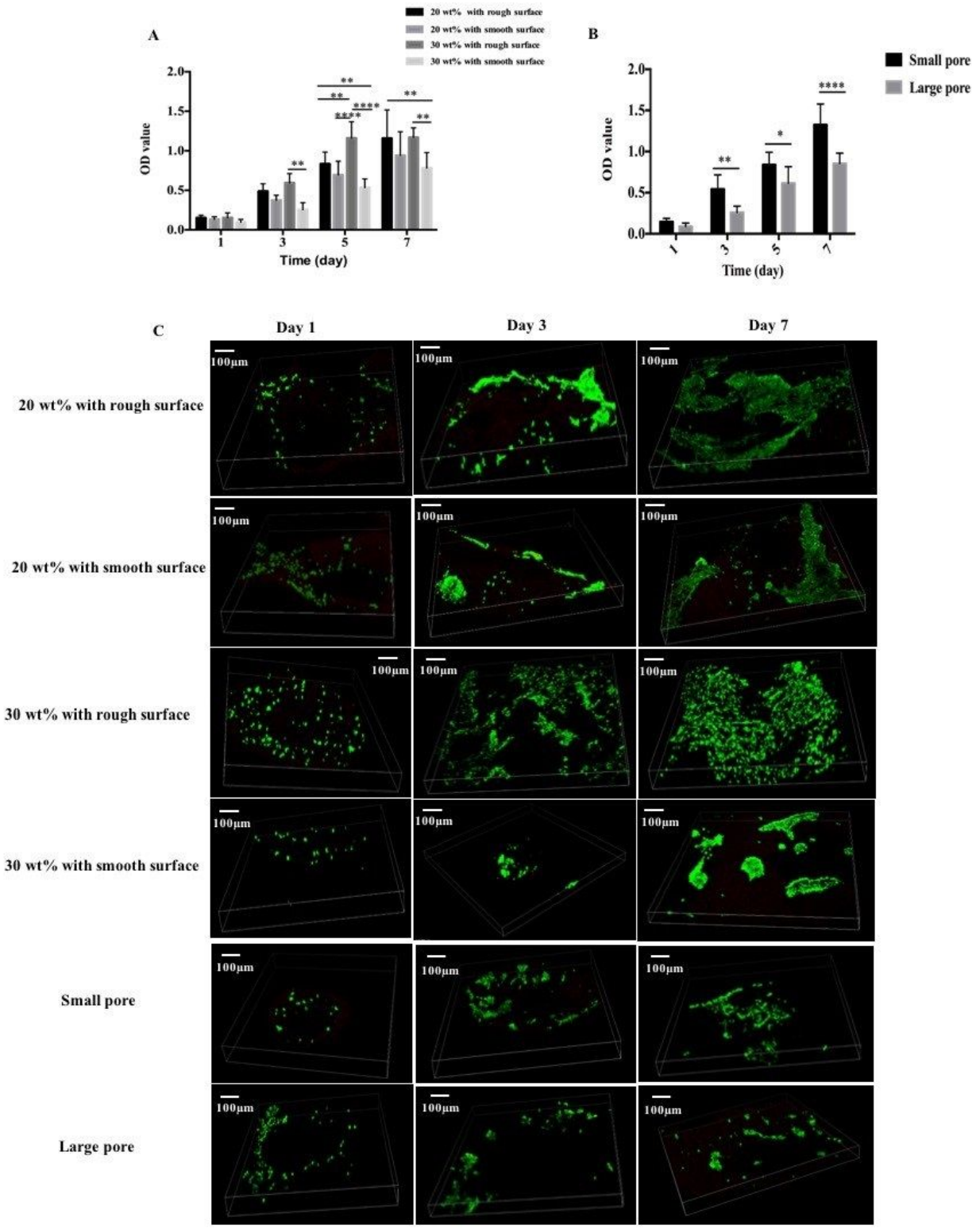

Figure 3

Cell proliferation and viability on different scaffolds. **A** cell proliferation on four types of scaffolds. **B** Cell proliferation on scaffolds with different pore sizes. **C** CLSM after Live/Dead staining of BEAS-2B cells on the surface of different SF/HPMC scaffolds at 1, 3, and 7 days, respectively. Green denotes Calcein-AM staining (staining live cells) of cells on scaffolds. Red denotes PI staining (staining dead cells) of cells on scaffolds.

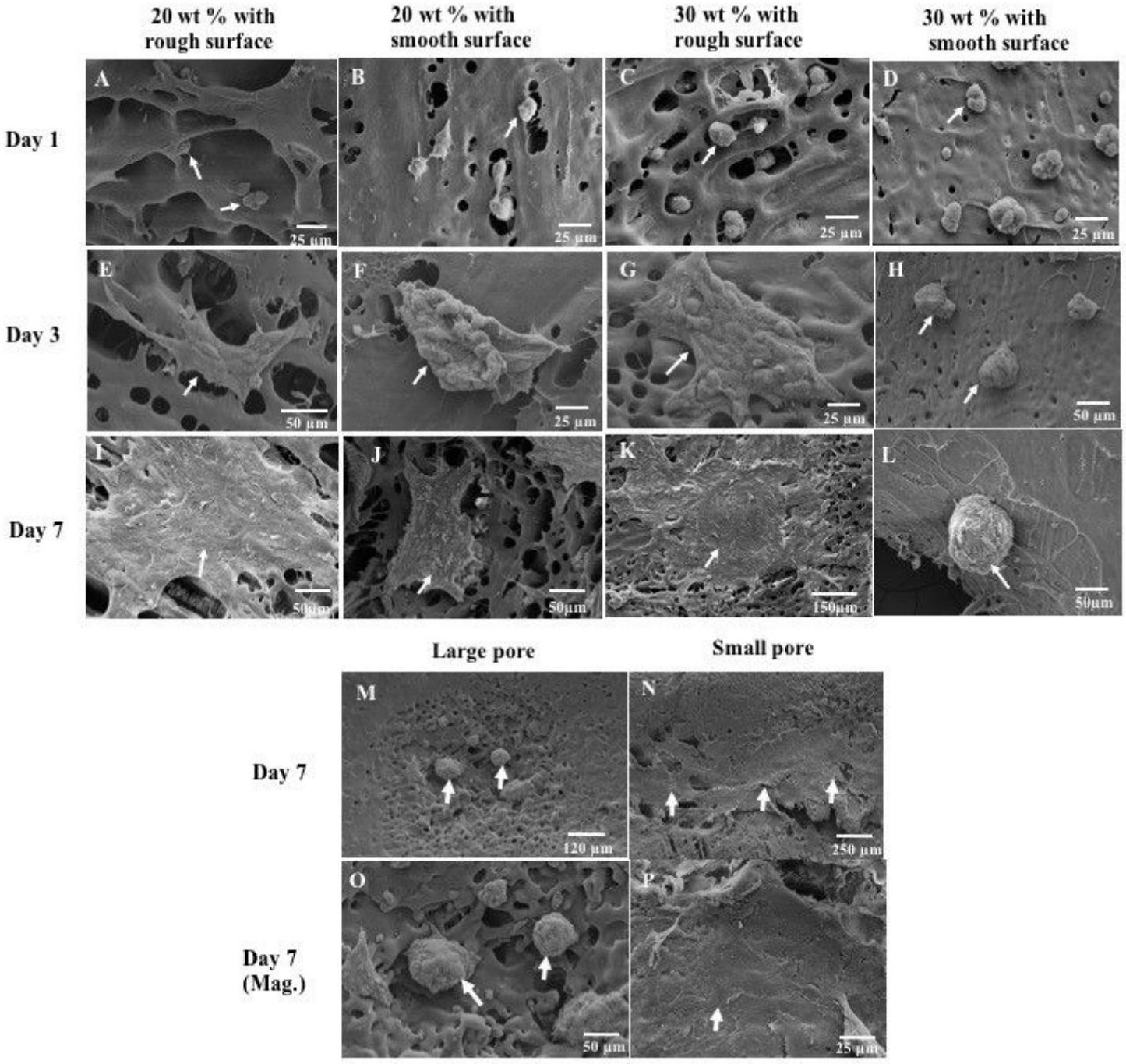

Figure 4

SEM images of BEAS-2B cells on the surface of different SF/HPMC scaffolds at 1, 3 and 7 days, respectively. **A-L** BEAS-2B cells morphology on the surface of different SF/HPMC scaffolds at 1, 3 and 7 days, respectively. **M-N** BEAS-2B cells morphology on the surface of 20 wt% SF/HPMC scaffolds with different pore size at 7 days. **O-P** Magnified images.